130 KSME Journal, Vol.5, No.2, pp. 130~139, 1991

HEAT TRANSFER OF A SPRAY DROPLET IN A PWR PRESSURIZER

Jong-Chull Jo,* Sang-Kyoon Lee* and Won-Ky Shin*

(Received July 16, 1991)

Heat transfer rates to spray droplets under conditions corresponding to those of spray transients in a pressurizer of pressurized water reactor (PWR) have been predicted by a simple droplet model with internal thermal resistance and partial internal mixing. In those processes, the temperature distributions in the droplet have been obtained using the integral method, and the physical properties of the saturated steam-hydrogen gas mixture surrounding the droplets are estimated applying the concept of compressibility factor and using appropriate correlations. Results have been provided for the temporal variations of total heat flux with its convection and condensation heat transfer components, dimensionless droplet bulk temperature and droplet flight distance. The effects of ambient pressure, initial droplet size, concentration of hydrogen gas in the mixture, initial injection velocity, and spray angle on the heat transfer of spray droplets have been discussed.

Key Words: Spray Droplet, PWR Pressurizer, Condensation Heat Transfer, Integral Method, Compressibility Factor

NOMENCLATURE

A : Cross-sectional area of a droplet
Bi : Biot number ($=h_t R/k_l$)
C_D : Drag coefficient
C_p : Specific heat at constant pressure
D : Derivative with respect to τ ($=d/d\tau$)
D_{12} : Mass diffusivity of steam in a mixture
g : Gravitational acceleration
H_{fg} : Latent heat of condensation
h_c : Convection heat transfer coefficient
h_t : Apparent heat transfer coefficient
J_s : Mass flux of steam
k : Thermal conductivity
M : Molecular weight
m : Mass of a droplet
Nu : Nusselt number ($=2h_c R/k_m$)
P : Pressure
P_{gm} : Logarithmic mean gas pressure difference
Pr : Prandtl number ($=\mu_m C_{pm}/k_m$)
q_L : Sensible heat flux to a droplet
q_S : Latent heat flux to a droplet
q_t : Total heat flux to a droplet
$\bar{R}$: Universal gas constant
Re : Reynolds number ($=2\rho_m WR/\mu_m$)
r : Radial distance in spherical coordinate
Sc : Schmidt number ($=\mu_m/D_{12}\rho_m$)
Sh : Sherwood number ($=2\beta R/D_{12}$)
T : Temperature
t : Time
U : Horizontal velocity component
V : Vertical velocity component
$\bar{V}$: Molar specific volume
v : Specific volume
W : Velocity of a droplet ($=(U^2+V^2)^{1/2}$)
x, y : Cartesian coordinates
Y : Flight distance
y_i : Volume fraction of each component in the mixture
Z : Compressibility factor
α : Thermal diffusivity
β : Mass transfer coefficient
Θ_b : Dimensionless droplet bulk temperature ($=(T_b-T_0)/(T_\infty-T_0)$)
θ : Transformed temperature in dimensionless form
μ : Dynamic viscosity
ξ : Dimensionless radial distance in spherical coordinate
ρ : Density
τ : Dimensionless time ($=\alpha_l t/R^2$)
ϕ : Spray angle
ω : Acentric factor

Subscripts

b : Bulk
c : Critical value
g : Noncondensable gas
i : At the interface between the droplet and the mixture
l : Droplet
m : Mixture
o : Initial condition
r : Reduced value
s : Saturated steam or droplet surface
∞ : Ambient

Superscript

o : Low pressure

*Korea Institute of Nuclear Safety P.O. Box 16, Daeduk-danji, Taejon 305-606, Korea

1. INTRODUCTION

A PWR pressurizer maintains the main coolant pressure within certain boundaries during normal operations and

limits pressure excursions during transients and hypothetical accidents. In operation, the pressurizer contains saturated steam-hydrogen gas (noncondensable) mixture and saturated water at a desired saturation temperature and pressure regulated by spray system, electrical heaters and relief valves. The function of the spray system is to prevent pressure increase by injecting subcooled water into the pressurizer vessel atmosphere to condense steam during volume surges causing pressure increases. The pressurizer spray droplets are projected at an angle from the spray nozzle with a high initial velocity and travel to either the pressurizer vessel interior wall or the surface of the saturated water, absorbing heat and mass from the mixture. A knowledge regarding the heat transfer and motion of pressurizer spray droplets is essential for overall analysis and design of the pressurizer spray system, and is a prerequisite for analyzing the transient thermal response of the pressurizer vessel wall.

The objective of this study is to predict the heat transfer rates and associated flight distances for pressurizer spray droplets during spray transients. Several studies on heat/mass transfer and/or hydrodynamics of droplet motion are involved in the literature (Clift, Grace and Weber, 1978). The condensation heat/mass transfer rates and the associated droplet fall heights for a spray droplet which is moving in air-steam mixtures with a flow Reynolds number $Re \leq O(10^2)$ have been theoretically and/or experimentally investigated by various authors (Kulic, Rhodes and Sullivan, 1975, Kulic and Rhodes, 1977, Chung and Ayyaswamy, 1977, Tanaka, 1980, Huang and Ayyaswamy, 1987a,b,c, Linn, Maskell and Patrick, 1988). The theoretical investigators (Kulic, Rhodes and Sullivan, 1975, Kulic and Rhodes, 1977, Chung and Ayyaswamy, 1977, Tanaka, 1980) have calculated the condensation heat transfer of spray droplets by three droplet models : the complete mixing model (the model without internal resistance), the partial mixing model (the model with internal resistance and internal circulation) and the non-mixing model (the model with internal resistance and no internal circulation), on the basis of the assumption that flow instabilities such as droplet oscillations and vortex shedding do not occur so that the moving spray droplets maintain the spherical shape. It is common to the theoretical analyses (Kulic, Rhodes and Sullivan, 1975, Kulic and Rhodes, 1977) that the complete mixing model and the non-mixing model yield different bounding values in the droplet bulk temperature response, and that the partial mixing model yields more realistic results.

During pressurizer spray transient, the flow Reynolds numbers of spray droplets translating in the mixture are in the range, $Re > O(10^2)$. For that range of flow Reynolds numbers, flow instabilities are known to occur and the deformation from the spherical shape of the droplet may be large (Clift, Grace and Weber, 1978), so that it is demanded to develope more realistic model with regards to the droplet shape. Furthermore realistic situations require the considerations of a spectrum of spray droplets of various size as well as the thermal and hydrodynamic interactions of moving droplets. However, for the present, it is very difficult to realistically simulate the hydrodynamics and the transport phenomena associated with condensation on the pressurizer spray droplet. Thus it is still important to attempt approximating the heat transfer rate to a pressurizer spray droplet and the associated droplet flight distance by a simplified method.

In this paper, the heat transfer rate to a pressurizer spray droplet and the associated flight distance are calculated using standard correlations for heat/mass transfer and drag of a rigid sphere, and the partial mixing model is used to describe the temperature field of the spray droplet. An analytical solution for the transient temperature distributions in a rigid sphere suddenly exposed to a convective heating, and subjected to a non-uniform initial temperature condition is obtained using the integral method (Özisik, 1980), and is applied to determine the temperature fields in the partial mixing model. Since the states of the saturated steam and the hydrogen gas, consisting the mixture at high pressure, are real-gas states, the physical properties of the mixture are estimated applying the concept of compressibility factor and using available empirical and/or semi-empirical correlations. The temperature dependency of physical properties of the droplet and ambient mixture is taken into account over whole flight time of a droplet. Typical results are provided for the temporal variations of total heat flux with its convection and condensation heat transfer components, dimensionless droplet bulk temperature and droplet flight distance, and the effects of ambient pressure, initial droplet size, concentration of the noncondensable, initial injection velocity, and spray angle on the heat transfer of a spray droplet are discussed.

2. THEORETICAL FORMULATION

2.1 Physical Model

Consider the introduction of a cold water droplet of radius R_0 and initial bulk temperature T_0 into the saturated steam-hydrogen gas mixture space in a PWR pressurizer. The droplet is projected with an initial velocity W_0 and at an angle ϕ_0 with respect to the vertical direction, as depicted schematically in Fig. 1. The ambient pressure P_∞, the corresponding saturation temperature T_∞, and the noncondensable concentration by volume $y_{g\infty}$ are taken to be prescribed. The spray droplet is colder than the mixture. Thus steam condensation occurs on the droplet surface and the spray droplet grows as it travels in the mixture space. In this study, the heat transfer and motion of the spray droplets are theoretically formulated assuming that the moving spray droplets maintain the spherical shape, the drag phenomena are those for rigid spheres, and the radiation heat transfer to the droplet from the mixture is negligible and the spray droplet induced flow of ambient gas mixture can be ignored.

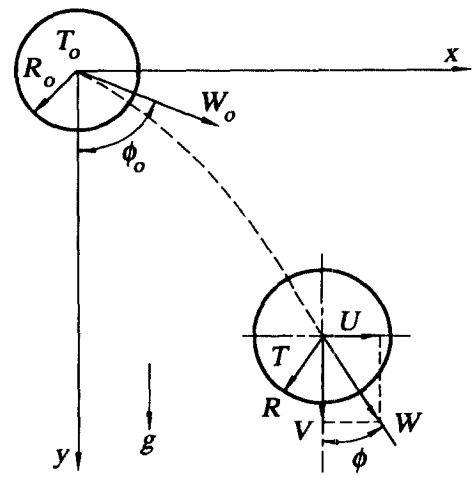

Fig. 1 Schematic of a spray droplet model.

2.2 Motion of a Spray Droplet

On the basis of the assumption that the drag phenomena for spray droplets are those for rigid spheres, the equation of motion and associated drag coefficients for spray droplet can be expressed as(Linn, Maskell and Patrick, 1988)

$$\frac{dU}{dt}=-C_D A\rho_m\frac{WU}{2m}-\frac{U}{m}\frac{dm}{dt} \tag{1}$$

$$\frac{dV}{dt}=g\frac{(\rho_l-\rho_m)}{\rho_l}-C_D A\rho_m\frac{WV}{2m}-\frac{V}{m}\frac{dm}{dt} \tag{2}$$

$$C_D=24/\mathrm{Re} \quad \text{for } \mathrm{Re}<2 \tag{3a}$$

$$C_D=18.197/\mathrm{Re}^{0.599} \quad \text{for } 2<\mathrm{Re}<500 \tag{3b}$$

$$C_D=0.44 \quad \text{for } 500<\mathrm{Re}<2\times10^5 \tag{3c}$$

The droplet trajectory is predicted from the Eqs.(1) ~ (3).

2.3 Heat and Mass Transfer to a Spray Droplet

The rates of condensation heat transfer from the mixture of saturated steam and noncondensable hydrogen gas to the spray droplet are calculated in this study using the simple model which was first expressed by Colburn and Hougen (1934) and subsequently used by various authors(Kulic, Rhodes and Sullivan, 1975, Kulic and Rhodes, 1977, Bergles et al., 1981). This model is that the total heat transfer from the mixture to the droplet surface is made up of two components ; firstly, the sensible (convection) heat transfer component caused by the temperature difference between the ambient mixture and the droplet surface and, secondly, the latent (condensation) heat transfer component caused by the steam concentration difference between the ambient mixture and the droplet-mixture interface. Thus, the total heat flux to the spray droplet in the steady state is given as

$$q_t=q_S+q_L \tag{4}$$

where

$$q_S=h_c a(T_\infty-T_s)/(1-e^{-a}) \tag{5}$$

$$q_L=J_s H_{fg} \tag{6}$$

$$a=J_s C_{ps}/h_c \tag{7}$$

The mass condensation flux of the steam J_s can be expressed as

$$J_s=\rho_s\beta(P_{gi}-P_{g\infty})/P_{gm} \tag{8}$$

where

$$P_{gm}=(P_{gi}-P_{g\infty})/\ln(P_{gi}/P_{g\infty}) \tag{9}$$

More details of the above derivations and pertinent assumptions can be found in refs.(Kulic, Rhodes and Sullivan, 1975, Kulic and Rhodes, 1977, Bergles et al., 1981). The convection heat transfer coefficient h_c in Eqs.(5), (7) and the mass transfer coefficient β in Eq.(8) are calculated, in this study, from the correlations proposed by Hughmark(1967).

$$\mathrm{Sh} \text{ or } \mathrm{Nu}=2.0+0.6\mathrm{Re}^{1/2}(\mathrm{Sc} \text{ or } \mathrm{Pr})^{1/3}$$
$$\text{for } 1<\mathrm{Re}<450,\ \mathrm{Sc} \text{ or } \mathrm{Pr}<250 \tag{10a}$$

$$\mathrm{Sh} \text{ or } \mathrm{Nu}=2.0+0.27\ \mathrm{Re}^{1/2}(\mathrm{Sc} \text{ or } \mathrm{Pr})^{1/3}$$
$$\text{for } 450<\mathrm{Re}<10^4,\ \mathrm{Sc} \text{ or } \mathrm{Pr}<250 \tag{10b}$$

These correlations are originally based on a large number of experimental heat and mass transfer data for spheres in the flow Reynolds number range $1<\mathrm{Re}<10^4$. In this study, Eq. (10b) is still used for the high Reynolds number range Re=O (10^4) on the basis of assumption that extrapolation of the Eq. (10b) is valid because neither correlation nor experimental data for $\mathrm{Re}>10^4$ is found to be available.

2.4 Droplet Temperature Reponse

While the non-mixing model implies that the droplet is assumed to be a rigid sphere, the partial mixing model simulates the droplet with internal mixing by assuming that the droplet behaves as a rigid sphere in which a finite number of instantaneous complete mixings occur periodically at an interval of the time taken for a specified droplet surface temperature increase. Hence a uniform initial temperature profile is obtained for each transient interval between any two consecutive time points at which the internal mixings occur. In order to obtain the droplet temperature responses for these models a boundary condition at the droplet surface is needed. The total heat flux at the droplet surface can be used to define an apparent heat transfer coefficient h_t expressed as

$$h_t=q_t/(T_\infty-T_s) \tag{11}$$

Then we can consider that the droplet surface is subjected to a convection heat transfer from the surroundings at the prescribed uniform temperature T_∞ into the droplet having a non-uniform initial temperature expressed by a n th-order polynomial with the apparent heat transfer coefficient h_t. Over sufficiently small increases in either the droplet surface temperature or the droplet bulk temperature, all the physical properties and the droplet radius can be considered to be constants. Thus the mathematical formulation of the problem considered herein for period of very small change in the droplet surface temperature, in the dimensionless form, can be expressed as

$$\frac{\partial^2\theta}{\partial\xi^2}=\frac{\partial\theta}{\partial\tau} \quad \text{in } 0<\xi<1,\ \tau>0 \tag{12}$$

$$\theta=F(\xi) \quad \text{for } \tau=0, \text{ in } 0\le\xi\le1 \tag{13}$$

$$\theta=0 \quad \text{at } \xi=0,\ \tau>0 \tag{14a}$$

$$\frac{\partial\theta}{\partial\xi}+(\mathrm{Bi}-1)\theta=0 \quad \text{at } \xi=1,\ \tau>0 \tag{14b}$$

where $F(\xi)$ is a n th-order polynomial. The dimensionless variables introduced in Eqs.(12) ~ (14) are defined as

$$\xi=\frac{r}{R},\ \tau=\frac{a_l t}{R^2},\ \theta=\frac{rT}{RT_\infty},\ \mathrm{Bi}=\frac{h_t R}{k_l} \tag{15}$$

Now this problem to be solved is the homogeneous linear problem of heat conduction in a slab with non-uniform initial temperature profile. In this study, Eqs.(12) ~ (14) are solved using the integral method. Admittedly, the solution of this problem will be valid only for the interval of sufficiently small change in the droplet surface temperature. Assuming that the solution of Eq. (12) can be expressed by a polynomial in the same form as the initial temperature profile

$$\theta(\xi,\tau)=\sum_{i=0}^{n}a_i(\tau)\xi^i \quad \text{in } 0<\xi<1,\ \tau>0 \tag{16}$$

$n+1$ relations are needed to determine the $n+1$ unknown coefficients $a_i(\tau)$, $(i=0,1,\cdots\cdots,n)$.

The two boundary conditions given by Eqs. (14) provide the two relations as follows

$$a_0(\tau)=0 \tag{17a}$$

$$a_n(\tau)=-\frac{\sum_{i=0}^{n-1}(\mathrm{Bi}+i-1)\,a_i(\tau)-\mathrm{Bi}}{(\mathrm{Bi}+n-1)} \tag{17b}$$

The $n-1$ additionals can be obtained by the moment method (Özisik, 1980). Multiplying Eq. (12) by a weight functions $g_j(\xi)$, $(j=1,2,\cdots,n-1)$ and integrating the resulting equation between $\xi=0$ and $\xi=1$, and then introducing Eq. (16) into the above-mentioned resulting equation yields

$$\sum_{i=2}^{n}a_i(\tau)\int_{\xi=0}^{1}i(i-1)\,g_j(\xi)\,\xi^{i-2}d\xi =\sum_{i=0}^{n}\frac{da_i(\tau)}{d\tau}\int_{\xi=0}^{1}g_j(\xi)\,\xi^i d\xi \tag{18}$$

Thus Eqs. (18) provide a system of $n-1$ linearly independent first order ordinary differential equations for the determination of the remaining $n-1$ coefficients. The $n-1$ initial conditions for solving Eqs. (18) are obtained by equating $n-1$ moments of $F(\xi)$ of Eq. (13) to the corresponding moments of $\theta(x,0)$ of Eq. (16), i.e.

$$\int_{\xi=0}^{1}g_j(\xi)\,F(\xi)\,d\xi=\sum_{i=1}^{n}a_i(0)\int_{\xi=0}^{1}g_j(\xi)\,\xi^i d\xi \tag{19}$$

Then the solution will become unique if the weight funcitions $g_j(\xi)$, $(j=1,2,\cdots,n-1)$ are specified. The weight functions used in this study are

$$g_j(\xi)=\xi^{j-1} \qquad j=1,2,\cdots,n-1 \tag{20}$$

The set of $n-1$ simultaneous linear first-order differential equations in $n-1$ unknown funcitions $a_i(\tau)$, $(i=1,2,\cdots,n-1)$ obtained by introducing Eq. (20) into Eq. (18) can be represented in the matrix form.

$$[\boldsymbol{L}]\{\boldsymbol{a}\}=\{\boldsymbol{h}\} \tag{21}$$

where the coefficient matrix of Eq. (21) $[\boldsymbol{L}]$ is the linear differential operator matrix whose elements are given by

$$L_{i,j}=B_{i,j}D+E_{i,j} \qquad \begin{matrix} i=1,2,\cdots,n-1 \\ j=1,2,\cdots,n-1 \end{matrix} \tag{22}$$

with

$$B_{i,j}=\frac{1}{i+j}-\frac{(\mathrm{Bi}+j-1)}{(n+i)\,(\mathrm{Bi}+n-1)} \tag{23}$$

and

$$E_{i,j}=\begin{cases}\dfrac{n(n-1)\,(\mathrm{Bi}+j-1)}{(n+i-2)\,(\mathrm{Bi}-n-1)} & \text{for } j=1 \qquad (24a)\\[2ex] \dfrac{n(n-1)\,(\mathrm{Bi}+j-1)}{(n+i-2)\,(\mathrm{Bi}+n-1)}-\dfrac{j(j-1)}{(i+j-2)} & \text{for } j=2,3,\cdots,n-1 \qquad (24b)\end{cases}$$

,and the elements of the forcing funcition matrix $\{\boldsymbol{h}\}$ are given by

$$h_i=\frac{n(n-1)\,\mathrm{Bi}}{(n+i-2)\,(\mathrm{Bi}+n-1)} \tag{25}$$

The characteristic equation for $a_i(\tau)$, $(i=1,2,\cdots,n-1)$ obtained by replacing D by λ in the expression for $|\boldsymbol{L}|=0$ is given as

$$\lambda^{n-1}+A_1\lambda^{n-2}+\cdots\cdots+A_{n-2}\lambda+A_{n-1}=0 \tag{26}$$

where the coefficients of Eq. (26) A_i, $(i=1,2,\cdots,n-1)$ are constants determined by the prescribed value of Bi. In this study, the general homogeneous solutions of Eq. (21) are obtained solving Eq. (26) by the Bairstow's method. The general solutions of Eq. (21) can be expressed in the form

$$a_i(\tau)=\sum_{j=1}^{n-1}C_{i,j}e^{-\lambda_j\tau}+a_{ip} \quad i=1,2,\cdots,n-1 \tag{27}$$

where $\lambda_j(j=1,2,\cdots,n-1)$ are the $n-1$ roots of Eq. (26) and $a_{ip}(i=1,2,\cdots,n-1)$ represents the particular solutions of Eq. (21). Substituting Eq. (27) into Eq. (21) for the purpose of obtaining conditions on the unknown constants $C_{i,j}$ $(i=1,2,\cdots,n-1\,;\,j=1,2,\cdots,n-1)$ in Eq. (27), all the unknown constants $C_{i,j}$ except $C_{1,j}$ can be expressed in terms of $C_{1,j}$.

$$C_{i,j}=f_{i,j}C_{1,j} \qquad \begin{matrix} i=2,3,\cdots,n-1 \\ j=1,2,\cdots,n-1 \end{matrix} \tag{28}$$

where the coefficients $f_{i,j}$ are known constants. Finally, the $n-1$ remaining unknown coefficients $C_{1,j}$ can be obtained by introducing Eq. (20), (27) and (28) into Eq. (19).

The droplet bulk temperature T_b is expressed as

$$T_b=\frac{3}{4\pi R^3}\int_0^R 4\pi T r^2 dr =3T_\infty\sum_{i=1}^{n}\frac{a_i(\tau)}{i+2} \tag{29}$$

and the droplet surface temperature T_s is expressed as

$$T_s=T_\infty\sum_{i=1}^{n}a_i(\tau) \tag{30}$$

2.5 Droplet Size Change

The above solution of the droplet temperature response has been derived on the basis of the assumption that the droplet radius is constant over a time period taken for a small surface temperature increase. This assumption in not quite true because the steam condensation on the droplet occurs continuously.

However the effect of a small change in the droplet radius on the temperature response of the droplet can be considered to be negligible. Thus the droplet radius change is accounted for by

$$\frac{d}{dt}(R^3)=\frac{3J_sR^2}{\rho_l} \tag{31}$$

and the increased radius during a time step is taken as the constant radius of the next time step.

2.6 Physical Properties of the Mixture

(1) Equation of State

The law of ideal gases no longer applies to both the saturated steam and hydrogen gas at higher pressures and/or near the condensing temperature. However the behavior of real gases can be related to that of ideal gases by introducing the compressibility factor expressed as

$$Z=\frac{P\overline{V}}{\overline{R}T} \tag{32}$$

The compressibility factor Z of real gases can be calculated using the following three-parameter correlation; the three parameters are the reduced temperature T_r, reduced pressure P_r and the acentric factor ω (Reid, Plausnitz and Sherwood, 1977).

$$Z=Z^{(0)}(T_r,P_r)+\omega Z^{(1)}(T_r,P_r) \tag{33}$$

The two terms $Z^{(0)}$, $Z^{(1)}$ as funcitions of T_r and P_r, and the acentric factor ω for both steam and hydrogen gas can be determined with tables and property data bank recorded in ref.(Reid, Plausnitz and Sherwood, 1977).

The reduced temperature and reduced pressure are defined as

$$T_r=\frac{T}{T_c},\ P_r=\frac{P}{P_c} \tag{34}$$

To apply the above method to the mixture of saturated steam and hydrogen gas, the pseudocritical values for the mixture are evaluated according to the modified Prausnitz and Gunn rules(Reid, Plausnitz and Sherwood, 1977).

$$T_{cm}=\sum_i y_i\ T_{ci} \tag{35a}$$

$$\overline{V}_{cm}=\sum_i y_i\overline{V}_{ci} \tag{35b}$$

$$Z_{cm}=\sum_i y_i Z_{ci} \tag{35c}$$

$$P_{cm}=\frac{Z_{cm}\overline{R}T}{\overline{V}_{cm}} \tag{35d}$$

$$\rho_{cm}=\frac{M_m}{\overline{V}_{cm}} \tag{35e}$$

where

$$M_m=\sum_i y_i M_i \tag{36}$$

The mixture acentric factor is given by

$$\omega_m=\sum_i y_i\omega_i \tag{37}$$

(2) Density

The density ρ_m and reduced density ρ_{rm} of the mixture are given by

$$\rho_m=\frac{1}{v_m}=\frac{M_m}{\overline{V}_m} \tag{38a}$$

$$\rho_{rm}=\frac{\rho_m}{\rho_{cm}}=\frac{\overline{V}_{cm}}{\overline{V}_m} \tag{38b}$$

(3) Thermal Conductivity

The thermal conductivity of the mixture at low pressure k_m^o is obtained by Brokaw's correlation(Brokaw, 1955),

$$k_m^o=Sk_{mL}^o+(1-S)k_{mR}^o \tag{39}$$

where

$$k_{mL}^o=\sum_i y_i k_i^o \tag{40a}$$

$$\frac{1}{k_{mR}^o}=\sum_i\frac{y_i}{k_i^o} \tag{40b}$$

and Brokaw factor S can be found in ref. (Brokaw, 1955).

The thermal conductivities of all gases increase with pressure, and most of all the correlations describing the effect of pressure on the thermal conductivity are based on the correlating technique suggested by Vargaftik(Reid, Plausnitz and Sherwood, 1977).

$$k_m-k_m^o=f(\rho_{rm}) \tag{41}$$

In this equation, the difference between thermal conductivity at high pressure and that at low pressure is a function of reduced density. Stiel and Thodos(1964) suggest correlations for the function $f(\rho_{rm})$ as

$$f(\rho_{rm})=14.0\times10^{-8}\{\exp(0.535\rho_{rm}-1)/\Gamma_m\ Z_{cm}^5\}\quad(\rho_{rm}<0.5) \tag{42a}$$

$$f(\rho_{rm})=13.1\times10^{-8}\{\exp(0.67\rho_{rm}-1.069)/\Gamma_m Z_{cm}^5\}\quad(0.5<\rho_{rm}<2.0) \tag{42b}$$

$$f(\rho_{rm})=2.976\times10^{-8}\{\exp(1.155\rho_{rm}+2.016)/\Gamma_m Z_{cm}^5\}\quad(2.0<\rho_{rm}<2.8) \tag{42c}$$

where

$$\Gamma_m=\frac{T_{cm}^{1/6}M_m^{1/2}}{P_{cm}^{2/3}} \tag{43}$$

(4) Specific Heat at Constant Pressure

In order to determine the specific heat at constant pressure of the mixture, the molar specific heat at constant pressure must be first evaluated by the followings.

$$C_{pm}^o=\sum_i y_i C_{pi}^o \tag{44}$$

Eq.(44) applies to an ideal gas, and the specific heat of a real gas at constant pressure is related to the value in the ideal gas state, at the same temperature and composition,

$$C_{pm}=C_{pm}^o+\Delta C_{pm} \tag{45}$$

where ΔC_{pm} is a residual specific heat at constant pressure; it can be determined by taking the partial derivative of the enthalpy departure at constant pressure and composition as

$$\Delta C_{pm}=\frac{\partial}{\partial T}(H-H^o)_{T,comp} \tag{46}$$

by the use of reduced temperature and pressure, ΔC_{pm} can be calculated form the Lee-Kesler(1975) method.

$$\Delta C_{pm}=\Delta C_{pm}^{(0)}(T_r,P_r)+\omega\Delta C_{pm}^{(1)}(T_r,R_r) \tag{47}$$

(5) Viscosity

The viscosity of the mixture at low pressure is calculated by Wilke's method(Reid, Plausnitz and Sherwood, 1977),

$$\mu_m^o=\sum_i\frac{y_i\mu_i^o}{\sum_j y_j\Psi_{ij}} \tag{48}$$

where

$$\Psi_{ij}=\frac{\{1+(\mu_i^o/\mu_j^o)^{1/2}(M_j/M_i)^{1/4}\}^2}{\{8(1+M_i/M_j)\}^{1/2}} \tag{49a}$$

$$\Psi_{ji}=\frac{\mu_j^o M_i}{\mu_i^o M_j}\Psi_{ij} \tag{49b}$$

The viscosity of the mixture at high pressure is calculated from the following correlation suggested by Dean and Steil

(1965),

$$(\mu_m-\mu_m^o)\,\xi_m=1.08\{\exp(1.439\rho_{rm})-\exp(-1.111\rho_{rm}^{1.858})\} \quad (50)$$

where

$$\xi_m=\frac{T_{cm}^{1/6}}{M_m^{1/2}P_{cm}^{2/3}} \quad (51)$$

(6) Mass Diffusivity

The mass diffusivity of the mixture is calculated from the correlation including the terms of the atomic diffusion volumes that is proposed by Fuller et al.(Reid, Plausnitz and Sherwood, 1977).

$$D_{12}^o=\frac{1.013\times10^{-7}T^{1.75}\{(M_i+M_j)/M_iM_j\}^{1/2}}{P\{(\Sigma V)_i^{1/3}+(\Sigma V)_j^{1/3}\}^2} \quad (52)$$

By introducing the values of the atomic diffusion vlumes, $(\Sigma V)_s=12.7$ and $(\Sigma V)_g=7.07$, and those of the molecular weight, $M_s=18.015$ and $M_g=2.016$, into the above equation

$$D_{12}^o=4.16037\times10^{-9}T^{1.75}/P \quad (53)$$

Since this equation is valid at low pressure, the mass diffusivity at high pressure is calculated from the following correlation suggested by Dawson, Khoury and Kobayashi (1970).

$$\frac{D_{12}\rho_m}{(D_{12}\rho_m)^o}=1+0.053423\rho_{rm}-0.030182\rho_{rm}^2-0.029725\rho_{rm}^3 \quad (54)$$

2.7 Calculation Procedure

In order to calculate the internal droplet temperature field, we assume stepwise small increases in the droplet surface temperature. The amount of each temperature increase ΔT_s is obtained by dividing the difference between the temperature of the mixture space and the initial droplet temperature by a sufficiently large number N so that the physical properties and the droplet radius can be considered to be constants over the small increase in the droplet surface temperature ΔT_s. This enables the evaluations of the mean vapor film temperature $(T_\infty+T_s)/2$, the corresponding physical properties and the heat and mass transfer coefficients given as Eq. (10). Thus an apparent heat transfer coefficient h_t can be determined from Eq.(11).

The transient temperature distributions in the droplet given by Eq. (16) are obtained by using the integral method described above. From Eq.(30) the time taken for the specified surface temperature increase is determined using the secant method. The calculation is performed until the difference between the calculated surface temperature and specified surface temperature meets a convergence criterion.

In this calculation process, the internal mixing is taken into account by specifing an uniform initial temperature profile determined from Eq.(29) at the beginning of each mixing period. The droplet radius change is determined from Eq.(31) and the new radius is used for the next time step. Finally, from the Eqs.(1)~(3) the droplet trajectory is predicted using a fourth order Runge-Kutta method. The physical properties of droplet are used corresponding values at the droplet bulk temperature. The whole calculation is repeated using a new assumed surface temperature increase until the droplet bulk temperature reaches the temperature of the ambient mixture.

3. RESULTS AND DISCUSSIONS

Throughout this paper, the number of 100 stepwise increases in the droplet surface temperature is used in all the numerical calculations. In the calculation process for the partial mixing droplet model, it is very important to choose the number of mixings adequately. It is indicated in refs. (Kulic and Rhodes, 1977, Clift, Grace and Weber, 1978) that the internal circulation velocity of droplet increases with the droplet size, with the flow Reynolds number and with the ratio of external to internal viscosity. A higher internal circulation velocity implies a larger number of mixings. Therefore, it can be said that the number of mixings is influenced by the droplet size, the flow Reynolds number and the ratio of external to internal viscosity. At the present, it is not possible to determine an optimum mixing number for any particular case since a detailed knowledge of the droplet internal circulation mechanism is not available in the literature. In ref.(Kulic and Rhodes, 1977), the authors arbitrarily have chosen the number ($n=35$) in their calculations. They have reported that the partial mixing model predictions agree closely with the experimental results over the whole range of experiments, but the predictions are underestimated for the cases of larger droplets. The means to the determination of the proper value of n used in this study is derived from the result of comparisons between predictions and experimental data(Kulic and Rhodes, 1977), on the basis of assumptions that the major factor of influencing the droplet internal circulation is the initial droplet size, and that the mixing number is directly proportional to the initial droplet size. In consequence, the value of n corresponding to the droplet radii covered in this study range from 35 to 45.

The representative of the comparisons between the present predictions and the experimental data for the dimensionless droplet bulk temperature Θ_b as a function of time is presented in Fig.2. Although some deviations of the partial mixing model predictions from the experimental results are found for the cases (b) and (d) in Fig.2, it can be generally said that the present predictions are in good agreement with the experimental data.

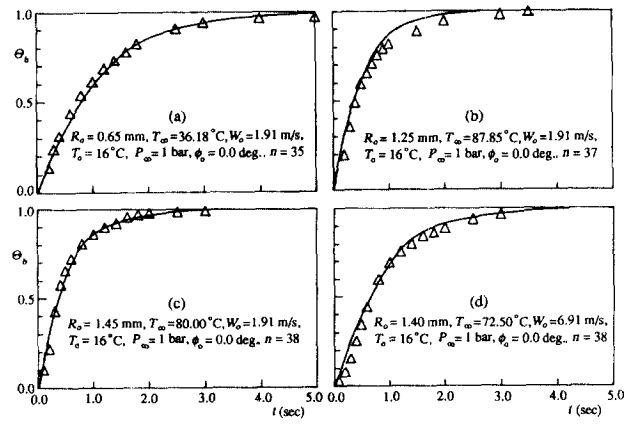

Fig. 2 Comparisons of calculation results with experimental data.
(△-Experimental data by Kulic & Rhodes, —— Present predictions)

In the subsequent paragraphs, we report the results calculated for spray droplets experiencing condensation in the PWR pressurizer. The parameter values used in the calculations are representative of the conditions in the pressurizer for the spray transients. The range of parameter values used in the calculations is ; pressurizer atmosphere pressure, P_∞= 50 to 155 ber ; initial radius of droplet, R_0=0.5 to 3.5mm ; noncondensable concentration by volume, $y_{g\infty}$=2 to 75% ; initial injection velocity of droplet, W_0=2 to 10m/s ; and spray angle, ϕ_0=0 to 52°. We provide the typical results obtained in terms of the temporal variations of total heat flux with its convection and condensation heat transfer components, dimensionless droplet bulk temperature and associated droplet flight distance for convenience, and discuss the effects of ambient pressure, initial droplet size, noncondensable concentration by volume, initial injection velocity and spray angle on the results.

Figs.3 and 4 show the effect of ambient pressure P_∞ on the heat transfer of a spray droplet. The volume fraction of noncondensable hydrogen $y_{g\infty}$ is maintained constant while the ambient pressure P_∞ is changed from 1 bar to 155 bar. The ambient temperature T_∞ is the saturation temperature at partial pressure of steam $(P_\infty - P_{g\infty})$ corresponding to prescribed values of both the ambient pressure P_∞ and the volume fraction of noncondensable $y_{g\infty}$. Fig.3 shows the temporal variations of total heat flux q_t, its sensible heat transfer component q_S and latent heat transfer component q_L. Fig.4 shows the temporal variations of dimensionless droplet bulk temperature Θ_b and droplet flight distance Y. With increasing ambient pressure P_∞, the sensible heat transfer component q_S increases while the latent heat transfer component q_L decreases. The reason is that the thermal driving force $(T_\infty - T_s)$ increases, but on the contrary the latent heat H_{fg} decreases with an increase of ambient pressure P_∞. Thus it is shown in Fig.3 that the major contribution to the interfacial heat flux comes from the latent heat transfer component at the ambient pressure of 1 bar, but comes from the sensible heat transfer component in the pressurizer pressure range of 50 bar to 155bar. With increasing ambient pressure P_∞, the total heat flux q_t increases, but the rate of increase of q_t decreases. The reason is that the rate of increase of q_S is lower than the rate of decrease of q_L. With an increase of ambient pressure, the droplet takes longer time to equilibrate with the ambient mixture due to the considerable reduction of the condensation heat transfer rate. The reason is that the difference between the ambient temperature and the initial temperature of droplet increase.

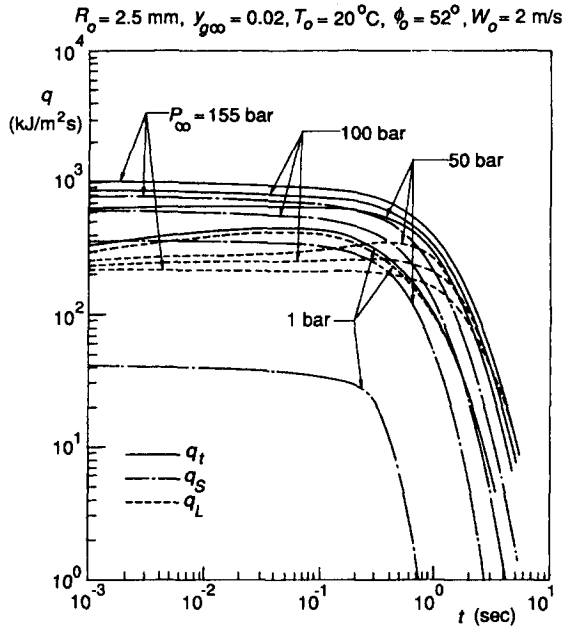

Fig. 3 The effect of ambient pressure on the heat flux to spray droplet.

Fig. 5 shows the effect of initial droplet size on the heat transfer of the spray droplet in terms of the temporal variations of dimensionless droplet bulk temperature and flight distance of the droplet. As shown in Fig.5, the bigger the droplet, the slower the increase of the dimensionless droplet bulk temperature and the longer the flight distance in which the droplet equilibrate with the environment. This is due to the fact that the ratio of the surface area available for heat transfer to the bulk volume of the droplet is inversely proportional to the droplet radius. And the bigger the droplet, the higher the terminal velocities as required by the drag-gravity force balance, so that the longer the flight distance at any given instant of time.

Figs.6 and 7 show the effect of volume fraction of noncondensable hydrogen gas on the heat transfer of the spray

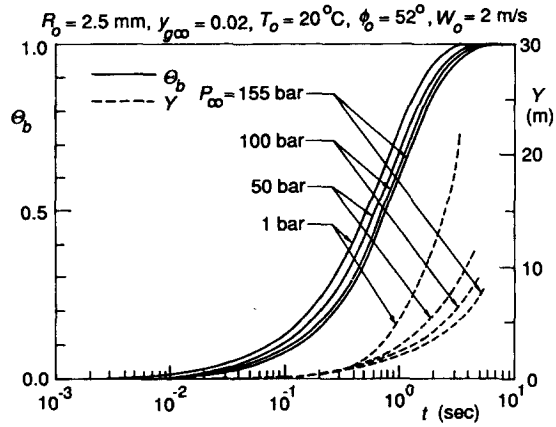

Fig. 4 The effect of ambient pressure on the bulk temperature and flight distance of spray droplet.

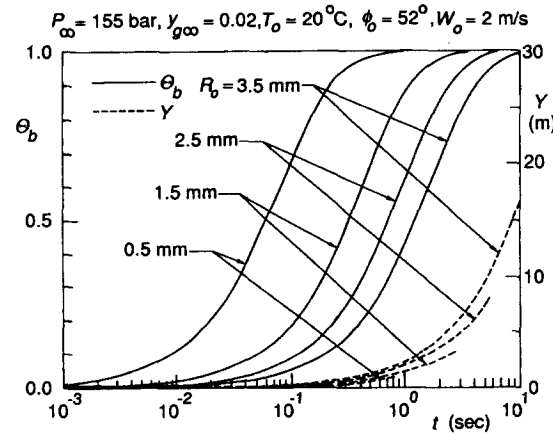

Fig. 5 The effect of initial droplet size on the bulk temperature and flight distance of spray droplet.

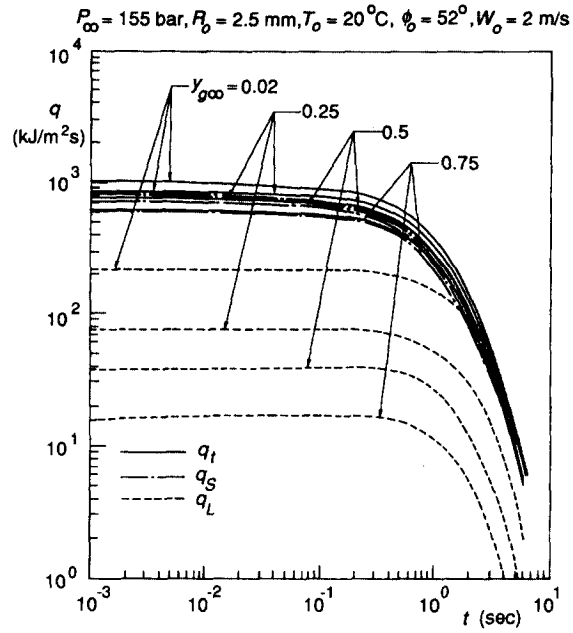

Fig. 6 The effect of volume fraction of noncondensable gas in mixture on the heat flux to spray droplet.

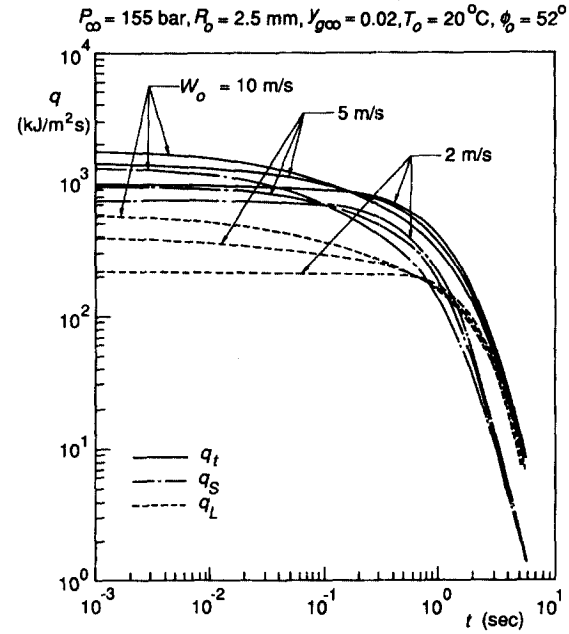

Fig. 8 The effect of initial droplet velocity on the heat flux to spray droplet.

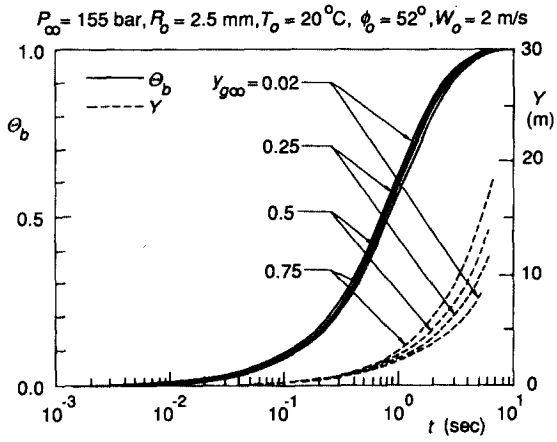

Fig. 7 The effect of volume fraction of noncondensable gas in mixture on the bulk temperature and flight distance of spray droplet.

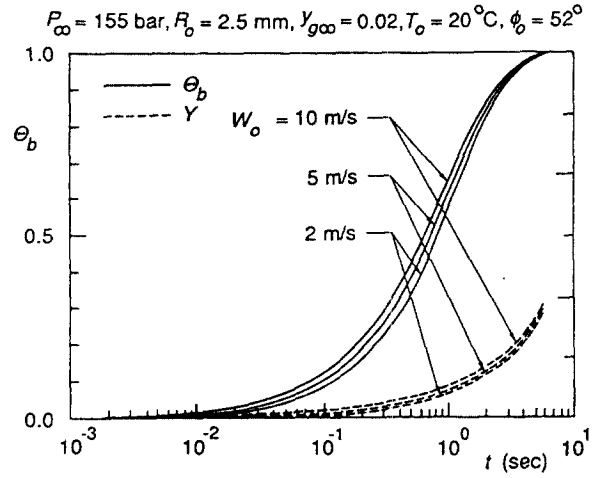

Fig. 9 The effect of initial droplet velocity on the bulk temperature and flight distance of spray droplet.

droplet. Fig.6 shows the results for the temporal variations of total heat flux q_t and its two heat transfer components, q_S and q_L, and Fig. 7 shows the results for the temporal variations of dimensionless droplet bulk temperature Θ_b and flight distance Y of the spray droplet. The ambient pressure P_∞ is maintained constant at 155 bar while the volume fraction of noncondensable hydrogen $y_{g\infty}$is changed from 0.02 to 0.75, and hence the ambient temperature (the steam saturation temperature) T_∞ is changed from 246.53℃ to 340.5℃. With increasing the volume fraction of noncondensable in the mixture, both the sensible heat transfer component q_S and the latent heat transfer component q_L decrease, and hence the dimensionless bulk temperature decreases at a faster rate. The reasons are that the existence of noncondensable gas acts as the external resistance to condensation heat transfer, and that the reduction of ambient temperature due to the existence of noncondensable gas results in the decrease of convection heat flux q_S. Fig.6 shows also that the rate of decrease of q_L is higher than that of q_S. The dependency of the dimensionless droplet bulk temperature on noncondensable concentration is not significant since the ratio of condensation heat transfer is small in the pressure range of pressurizer being considered herein. It is shown in Fig. 7 that, with an increase of noncondensable concentration, the droplet flight distance before reaching thermal equilibrium increases. This feature is identical with those observed in ref. (Tanaka, 1980) of which the results were obtained by using the drag coefficient appropriate for a rigid sphere in the calculations in the same manner as done in this study, but is opposite to the observed in ref. (Huang and Ayyaswamy, 1987a). It is known that there is a large pressure recovery in the rear of a moving droplet experiencing condensation (Sundararajan and

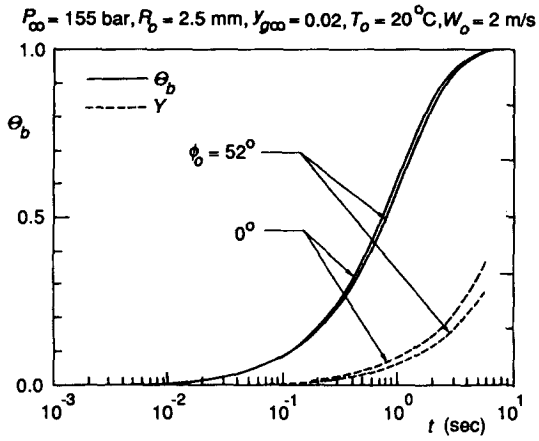

Fig. 10 The effect of spray angle on the bulk temperature and flight distance of spray droplet.

Ayyaswamy, 1984, Huang and Ayyaswamy, 1987b) so that the behavior of total drag coefficient is changed(Huang and Ayyaswamy, 1987c), and with increasing the condensation rate, the total drag coefficient decreases. Thus it is pointed out in ref. (Huang and Ayyaswamy, 1987a) that, in direct contact heat transfer calculations associated with moving droplet, the results obtained using the drag coefficient appropriate for a rigid sphere may be inaccurate. But as stated above, to calculate the drag associated with a spray droplet experiencing condensation accurately is very difficult at present stage and is beyond the scope of this study.

Figs.8 and 9 show the effect of initial velocity of a spray droplet on the spray droplet heat transfer. The ambient pressure and the initial radius of droplet in Fig. 8 are 155 bar and 2.5mm respectively. The higher the initial velocity, the larger the total heat transfer rates to a spray droplet as shown in Fig.8 and hence the faster the rate of dimensionless bulk temperature rise of a droplet as shown in Fig.9, and the longer the flight distance of a droplet before reaching thermal equilibrium. The dependency of droplet flight distance on the initial veclocity in a high ambient pressure as being considered in this study is small since the flight velocity of droplet is rapidly reduced to terminal velocity due to high drag force.

Fig. 10 shows the effect of droplet spray angle on the heat transfer. It is seen that the effect of spray angle on the rate of dimensionless droplet bulk temperature variation is small. However the droplet flight distance before reaching thermal equilibrium changes significantly with the spray angle. With increasing the spray angle, the dimensionless droplet bulk temperature decreases at very slow rate, and the flight distance decreases at a faster rate.

4. CONCLUSIONS

Heat transfer rates to spray droplets under conditions corresponding to those of spray transients in a PWR pressurizer have been predicted by the partial mixing model with both internal thermal resistance and partial internal mixing. An analytical solution of transient temperature distributions in a rigid sphere suddenly exposed to a convective heating, and subjected to a nonuniform initial temperature condition has been obtained using the integral method, and utilized to the calculations of temperature fields in the partial mixing droplet model. The physical properties of the saturated steam-noncondensable hydrogen gas mixture of pressurizer atmosphere have been estimated applying the concept of compressibility factor and using appropriate correlations. The temperature dependency of physical properties of the droplet and ambient mixture is taken into account over whole flight time of a droplet before attaining thermal equilibrium with the pressurizer atmosphere.

Unfortunately, available experimental data relevant to this study are only limited in the literature at present. Therefore the method for predicting the heat transfer rate to a spray droplet experiencing condensation, presented in this paper has been only partially validated by comparisons of the present results with available experimental data for the case that the ambient pressure is maintained constant at 1 bar.

Results have been provided for the temporal variations of total heat flux with its convection and condensation heat transfer components, dimensionless droplet bulk temperature and associated droplet flight distance, and for the effects of ambient pressure, initial droplet size, noncondensable concentration in the mixture, initial injection velocity, and spray angle. The results presented in this paper are considered to be useful as a prerequisite of the overall analysis and design of the pressurizer spray systems.

REFERENCES

Bergles, A.E., Collier, J.C., Delhaye, J.M., Hewitt, G.F. and Mayinger, F., 1981, "Two Phase Flow and Heat Transfer in the Power and Process Industries," Hemisphere Publishing Co., New York.

Brokaw, R.S., 1955, "Estimating Thermal Conductivities for Nonpolar Gas Mixtures," Ind. Eng. Chem., Vol.47, No.11, pp.2398~2400.

Chung, J.N. and Ayyaswamy, P.S., 1977, "The Effect of Internal Circulation on the Heat Transfer of a Nuclear Reactor Containment Spray Droplet," Nuclear Technology, Vol.35, pp.603~610.

Clift, R., Grace, J.R. and Weber, M.E., 1978, "Bubbles, Drops, and Particles," Academic Press., New York.

Colburn, A.P. and Hougen, O.A., 1934, "Design of Cooler Condensers for Mixture of Vapours with Non Condensing Gases," Ind. Eng. Chem., Vol.26, pp.1178~1182.

Dawson, R., Khoury, F. and Kobayashi, R., 1970, "Self-Diffusion Measurements in Methane by Pulsed Nuclear Magnetic Resonance," AIChE J., Vol.16, No.5, pp.725~729.

Dean, D.E. and Stiel, L.I., 1965, "The Viscosity of Nonpolar Gas Mixture at Moderate and High Pressures," AIChE J., Vol.11, No.3, pp.526~532.

Huang, L.J. and Ayyaswamy, P.S., 1987a, "Heat Transfer of a Nuclear Reactor Containment Spray Drop," Nuclear Engineering and Design, Vol.101, pp.137~148.

Huang, L.J. and Ayyaswamy, P.S., 1987b, "Heat and Mass Transfer Associated with a Spray Drop Experiencing Codensation : A Fully Transient Analysis," Int. J. Heat Mass Transfer, Vol.30, No.5, pp.881~891.

Huang, L.J. and Ayyaswamy, P.S., 1987c, "Drag Coefficients Associated with a Liquid Drop Experiencing Condensation," ASME J. Heat Transfer, Vol.109, pp.1003~1006.

Hughmark, G.A., 1967, "Mass and Heat Transfer from Rigid Sphere," AIChE Journal, Vol.13, No.6, pp.1219~1221.

Kulic, E., Rhodes, E. and Sullivan, G., 1975, "Heat Transfer Rates Predictions in Condensation on Droplets From Air-

Steam Mixtures," Can. J. Chemical Engineering, Vol.53, pp. 252~258.

Kulic, E. and Rhodes, E., 1977, "Direct Contact Condensation from Air-Steam Mixtures on a Single Droplet," Can. J. Chemical Engineering, Vol.55, pp.131~137.

Lee, B.I. and Kesler, M.G., 1975, "A Generalized Thermodynamic Correlation Based on Three-Parameter Corresponding States," AIChE J., Vol.21, No.3, pp.510~527.

Linn, J.D.M., Maskell, S.J. and Patrick, M.A., 1988, "A Note on Heat and Mass Transfer to a Spray Droplet," Nuclear Technology, Vol.81, pp.122~125.

Özisik, N., 1980, "Heat Conduction," John Wiley Sons Inc., New York.

Reid, R.D., Prausnitz, J.M. and Sherwood, T.K., 1977, "The Properties of Gases and Liquids," 3rd ed., McGraw-Hill Book Company, New York.

Stiel, L.I. and Thodos, G., 1964, "The Thermal Conductivity of Nonpolar Substances in the Dense Gaseous and Liquid Regions," AIChE J., Vol.10, No.1, pp.26~30.

Sundararajan, T. and Ayyaswamy, P.S., 1984, "Hydrodynamics and Heat Transfer Associated with Condensation of a Moving Drop : Solutions for Intermediate Reynolds Numbers," J. Fluid Mech., Vol.149, pp.33~58.

Tanaka, M., 1980, "Heat Transfer of a Spray Droplet in a Nuclear Reactor Containment," Nuclear Technology, Vol.47, pp.268~281.